

Supporting Information

Cu²⁺ complex of hydrophilic nitrogen-rich polymer dots applied as a new MRI contrast agent

**Mengyue Hu,^a Jing Chen,^{a,b} Jingmin Wang^a, Ye Zhang,^a Li Liu,^a Paulo Cesar Morais^{a,c} and
Hong Bi^{*a}**

a School of Chemistry and Chemical Engineering, Anhui University, Hefei 230601, P. R. China.

b Hefei Normal University, School of Life Sciences, Hefei 230601, P. R. China

c Universidade de Brasília, Instituto de Física, Brasília DF 70910-900, Brazil

**Corresponding author: Fax/Tel: +86 551 63861279; E-mail: bihong@ahu.edu.cn*

1. Quantum Yield (QY) Measurement

Table S2 QY of the fluorescent PVIm dots obtained at different ratio of VIm to water, $\lambda_{\text{ex}} = 360$ nm.

Table S3 QY of the fluorescent PVIm dots obtained at different hydrothermal temperature, $\lambda_{\text{ex}} = 360$ nm.

Table S4 QY of the fluorescent PVIm dots obtained after different hydrothermal times, $\lambda_{\text{ex}} = 360$ nm.

2. Supplemental Figures of the PVIm dots

Fig. S1 A typical TEM image of the Cu²⁺-PVIm dots complexes (the inset is the size distribution of the Cu²⁺-PVIm dots complexes).

Fig. S2 The DLS particle size distribution of the PVIm dots in (a) H₂O, (b) DMF, (c) MeOH, and (d) EtOH.

Fig. S3 FT-IR spectra of the PVIm dots, the PVIm and the monomer of VIm.

Fig. S4 XRD patterns of the PVIm dots at different reaction condition, (a) at different monomer concentrations; (b) after different hydrothermal temperature; (c) after different hydrothermal times.

Fig. S5 (a) XPS survey spectrum; XPS (b) C1s and (c) N1s spectra of the PVIm dots.

Fig. S6 PL emission spectra of the PVIm dots, the inset figure was normalized PL emission spectra. Excitation wavelengths started from 300 nm and increase with 10 nm increments, $\lambda_{\text{ex}} = 320$ nm.

Fig. S7 PL emission spectra of the PVIm dots in different solvents, $\lambda_{\text{ex}} = 320$ nm.

Fig. S8 PL emission spectra of the PVIm dots in different temperatures of the aqueous medium, $\lambda_{\text{ex}} = 320$ nm.

Fig. S9 PL emission spectra of the PVIm dots in aqueous solution with different pH value, $\lambda_{\text{ex}} = 320$ nm.

Fig. S10 PL emission spectra of PVIm dots at different NaCl solution, the concentration is 0, 5, 50, 100, 200, 300, and 400 mM, $\lambda_{\text{ex}} = 320$ nm.

Fig. S11 PL emission spectra of the PVIm dots solution at different concentrations, the inset

figure was normalized PL emission spectra, $\lambda_{\text{ex}} = 320$ nm.

Fig. S12 UV-Vis absorption spectra of the PVIIm dots at different reaction condition, (a) at different monomer concentrations; (b) after different hydrothermal temperature; (c) after different hydrothermal times.

Fig. S13 PL emission spectra of the PVIIm dots under different reaction condition, (a) at different monomer concentrations; (b) after different hydrothermal temperature; (c) at different hydrothermal times, $\lambda_{\text{ex}} = 320$ nm.

3. Supplemental Figures of Cu^{2+} -PVIIm dots complexes

Fig. S14 UV-Vis absorption spectra of Cu^{2+} -PVIIm dots upon addition of CuCl_2 in ultra-water: $[\text{CuCl}_2] = 0 \mu\text{M}$ to $500 \mu\text{M}$.

Fig. S15 The detection limit of the PVIIm dots coordinated with Cu^{2+} .

Fig. S16 Fluorescence responses of the PVIIm dots to different metal ions at concentration of $80.0 \mu\text{M}$, respectively. PVIIm dots: 0.2 mg mL^{-1} , $\lambda_{\text{ex}} = 320$ nm.

Fig. S17 Plots of $1/T_1$ vs. PVIIm dots. T_1 values were obtained at 0, 0.2, 0.4, 0.6, 0.8, 1, 2, and 3 mg mL^{-1} aqueous solution of the PVIIm dots, respectively.

Fig. S18 Plots of $1/T_2$ vs. concentration of Cu^{2+} added to 0.2 mg mL^{-1} aqueous solution of PVIIm dots to form complexes.

Table S1 The abbreviation of the obtained PVIIm dots at different hydrothermal reaction conditions

Ratio of VIm to water (v/v)	Hydrothermal temperature (°C)	hydrothermal time (h)	abbreviation for product
3/27	220	24	PVIIm dots
1/29	220	24	PVIIm dots-1
2/28	220	24	PVIIm dots-2
4/26	220	24	PVIIm dots-3
3/27	160	24	PVIIm dots-4
3/27	180	24	PVIIm dots-5
3/27	200	24	PVIIm dots-6
3/27	220	3	PVIIm dots-7
3/27	220	6	PVIIm dots-8
3/27	220	12	PVIIm dots-9

1. Quantum yield (QY) measurements

The quantum yield (QY) of fluorescent PVIIm dots was obtained by the following steps. We chose quinine sulfate dissolved in $0.1 \text{ M H}_2\text{SO}_4$ (literature quantum yield 0.54 at 360 nm) as reference. Then UV-vis absorption and PL emission spectra (with 360 nm excitation) of PVIIm dots and reference were measured respectively. The accurate QY value was calculated according to the given equation:

$$\Phi_{\text{sam}} = \Phi_{\text{ref}} \frac{I_{\text{sam}} A_{\text{ref}} \left(\frac{n_{\text{sam}}}{n_{\text{ref}}} \right)^2}{I_{\text{ref}} A_{\text{sam}} \left(\frac{n_{\text{ref}}}{n_{\text{sam}}} \right)^2}$$

In here “sam” and “ref” refer to sample and reference respectively. Q means Quantum yield. I is the integrated emission intensity, which could be calculated from the emission spectra at 360 nm excitation. A represents UV-Vis absorbance at 360 nm were control under 0.1 in the 10 mm quartz absorbance cell to avoid re-absorption effect. And n is the refractive index with 1.33 as the default for both quinine sulfate and PVIIm dots solvent.

Table S2 QY of the fluorescent PVIIm dots obtained at different ratio of VIm to water, $\lambda_{\text{ex}} = 360$ nm.

Sample	Intergrated emission intensity (I)	UV Absorbance	Refractive index of solvent (n)	QY
Quinine sulfate	17964.55	0.057	1.33	0.54
PVIIm dots-1	15432.51	0.055	1.33	0.48
PVIIm dots-2	14190.09	0.054	1.33	0.45
PVIIm dots-3	10164.93	0.052	1.33	0.33
PVIIm dots	16332.98	0.048	1.33	0.58

Table S3 QY of the fluorescent PVIIm dots obtained at different hydrothermal temperature, $\lambda_{\text{ex}} = 360$ nm.

Sample	Intergrated emission intensity (I)	UV Absorbance	Refractive index of solvent (n)	QY
Quinine sulfate	17964.55	0.057	1.33	0.54
PVIIm dots-4	3851.70	0.050	1.33	0.13
PVIIm dots-5	8549.09	0.046	1.33	0.32
PVIIm dots-6	17092.56	0.051	1.33	0.57
PVIIm dots	16332.98	0.048	1.33	0.58

Table S4 QY of the fluorescent PVIIm dots obtained after different hydrothermal times, $\lambda_{\text{ex}} = 360$ nm.

Sample	Intergrated emission intensity (I)	UV Absorbance	Refractive index of solvent (n)	QY
Quinine sulfate	17964.55	0.057	1.33	0.54
PVIIm dots-7	6668.55	0.052	1.33	0.22
PVIIm dots-8	6790.32	0.050	1.33	0.23
PVIIm dots-9	11324.81	0.052	1.33	0.37
PVIIm dots	16332.98	0.048	1.33	0.58

2. Supplemental Figures of the PVIm dots

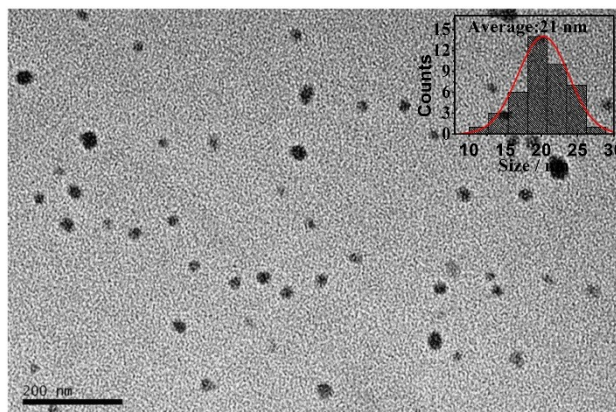


Fig. S1 A typical TEM image of the Cu²⁺-PVIm dots complexes (the inset is the size distribution of the Cu²⁺-PVIm dots complexes).

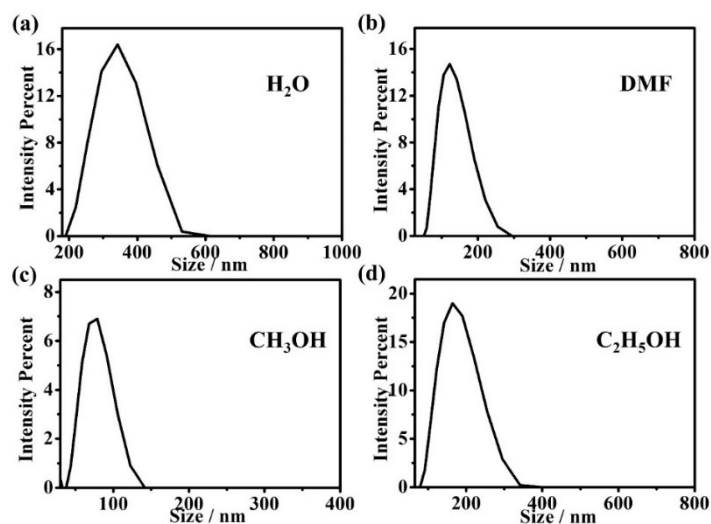


Fig. S2 The DLS particle size distribution of the PVIm dots in (a) H₂O, (b) DMF, (c) MeOH, and (d) EtOH.

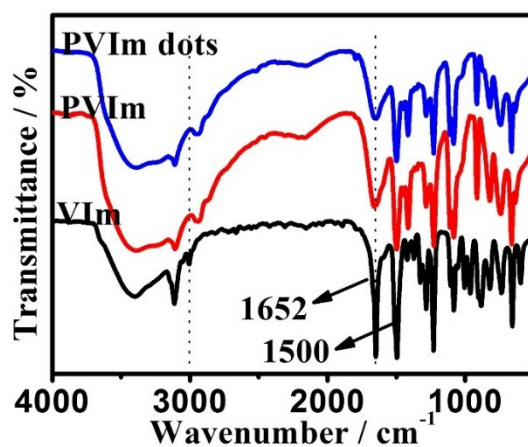


Fig. S3 FT-IR spectra of PVIm dots, PVIm and the monomer of VIm.

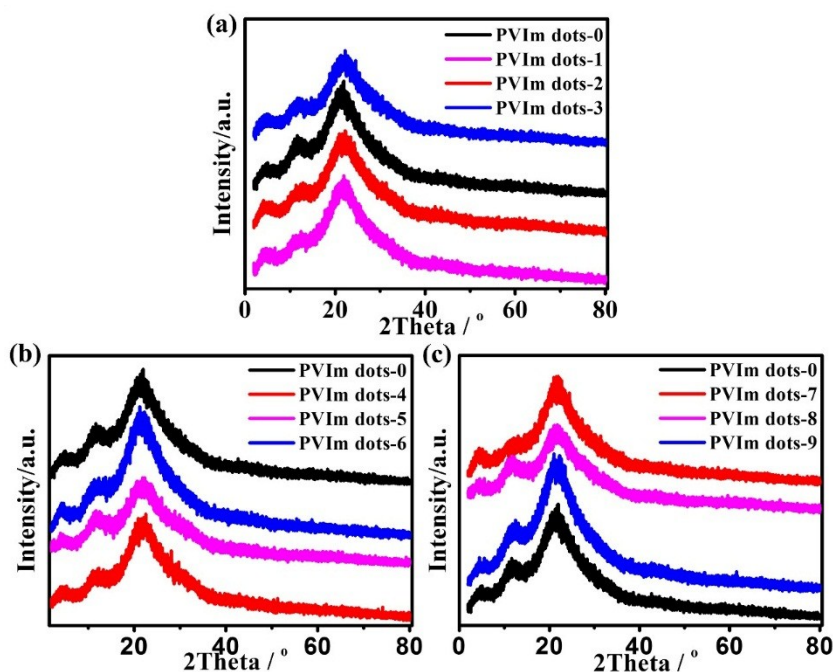


Fig. S4 XRD patterns of the PVIm dots at different reaction condition, (a) at different monomer concentrations; (b) after different hydrothermal temperature; (c) after different hydrothermal times.

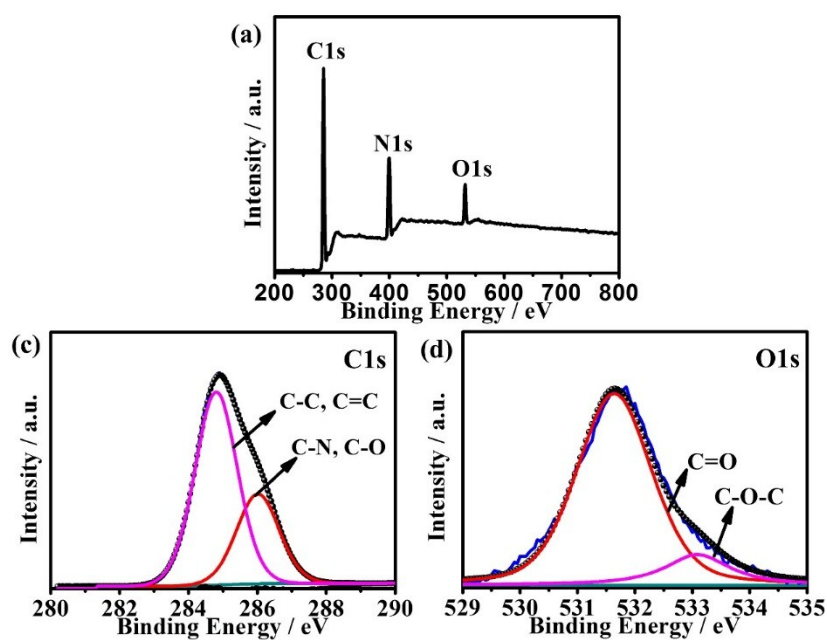


Fig. S5 (a) XPS survey spectrum; XPS (b) C1s and (c) N1s spectra of the PVIm dots.

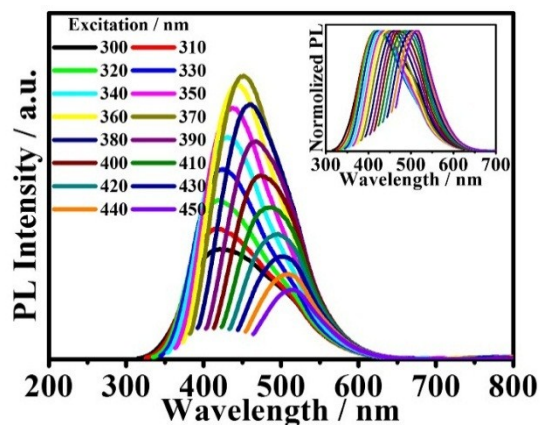


Fig. S6 PL emission spectra of the PVIIm dots, the inset figure was normalized PL emission spectra. Excitation wavelengths started from 300 nm and increase with 10 nm increments, $\lambda_{\text{ex}} = 320$ nm.

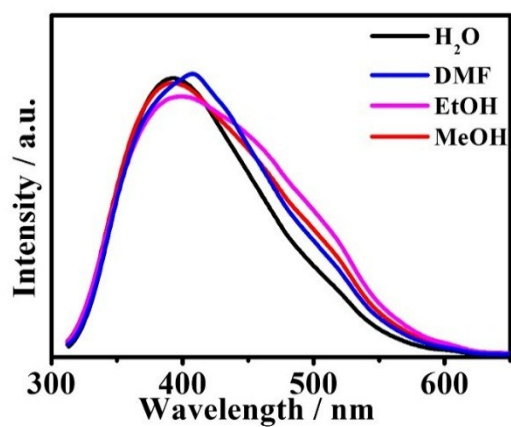


Fig. S7 PL emission spectra of the PVIIm dots in different solvents, $\lambda_{\text{ex}} = 320$ nm.

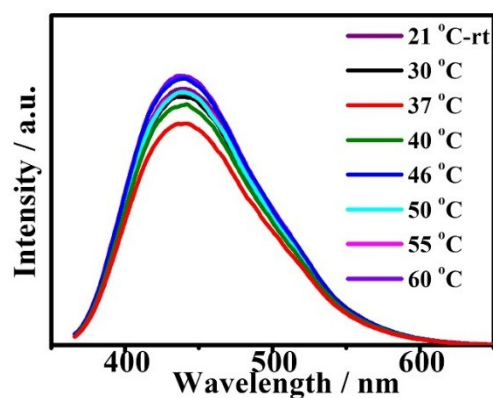


Fig. S8 PL emission spectra of the PVIIm dots in different temperatures of the aqueous medium, $\lambda_{\text{ex}} = 320$ nm.

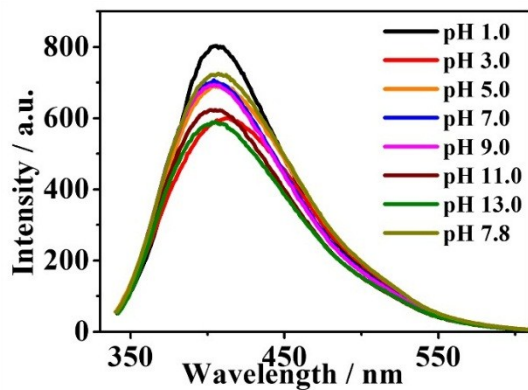


Fig. S9 PL emission spectra of the PVIIm dots in aqueous solution with different pH value, $\lambda_{\text{ex}} = 320$ nm.

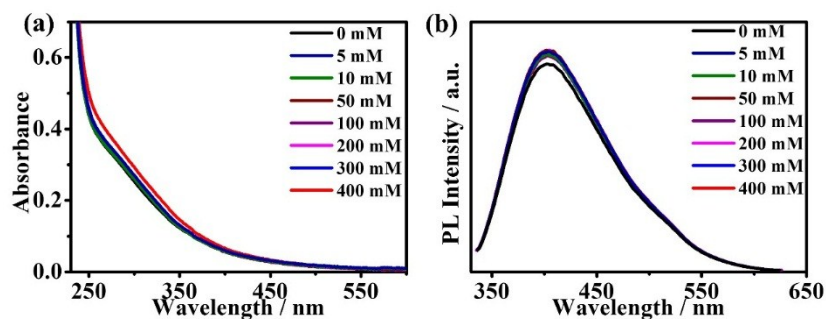


Fig. S10 PL emission spectra of PVIIm dots at different NaCl solution, the concentration is 0, 5, 50, 100, 200, 300, and 400 mM, $\lambda_{\text{ex}} = 320$ nm.

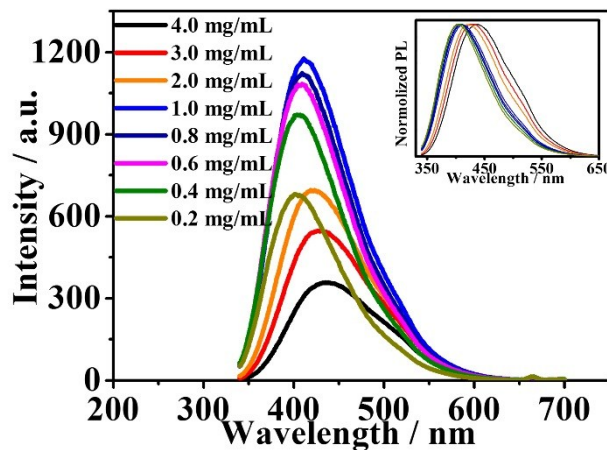


Fig. S11 PL emission spectra of the PVIIm dots solution at different concentrations, the inset figure was normalized PL emission spectra, $\lambda_{\text{ex}} = 320$ nm.

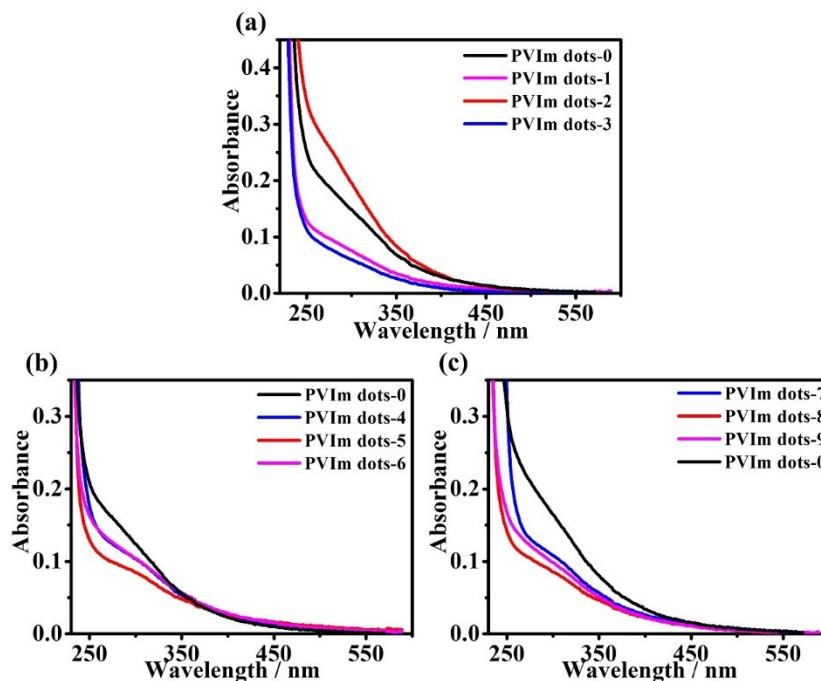


Fig. S12 UV-Vis absorption spectra of the PVIm dots at different reaction condition, (a) at different monomer concentrations; (b) after different hydrothermal temperature; (c) after different hydrothermal times.

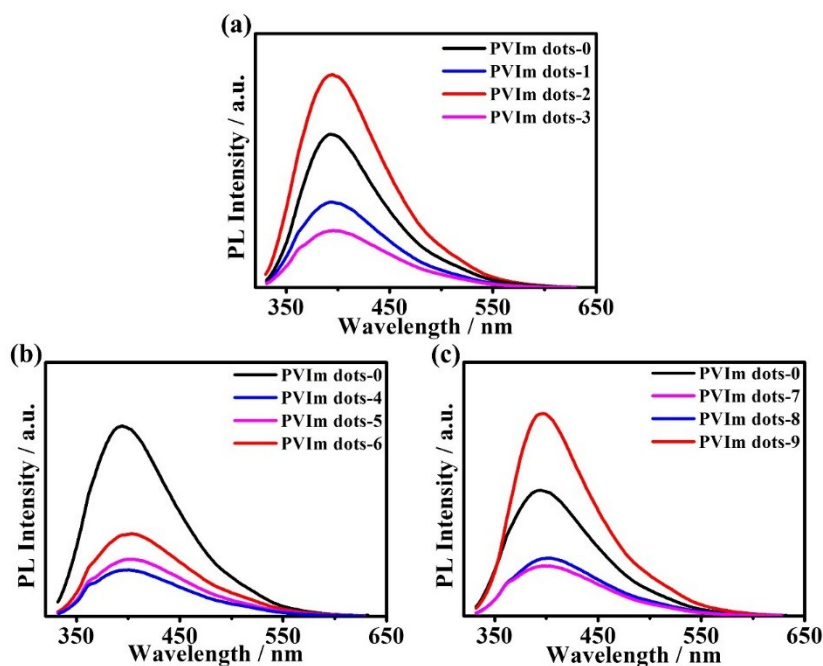


Fig. S13 PL emission spectra of the PVIm dots under different reaction conditions, (a) at different monomer concentrations; (b) after different hydrothermal temperature; (c) at different hydrothermal times, $\lambda_{\text{ex}} = 320 \text{ nm}$.

3. Supplemental Figures of the Cu^{2+} -PVIm dots complex and the

relaxivity of the PVIm dots

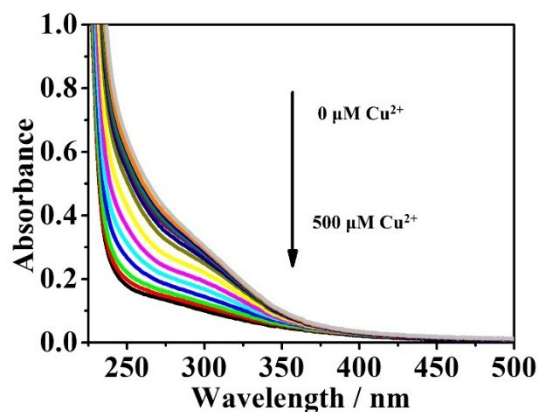


Fig. S14 UV-Vis absorption spectra of Cu^{2+} -PVIm dots upon addition of CuCl_2 in ultra-water: $[\text{CuCl}_2] = 0 \mu\text{M}$ to $500 \mu\text{M}$.

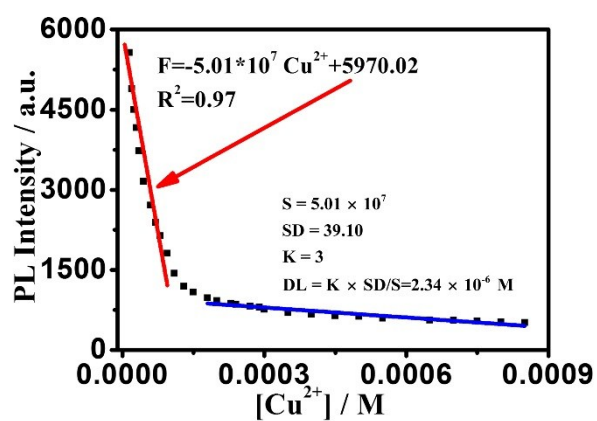


Fig. S15 The detection limit of the PVIm dots coordinated with Cu^{2+} .

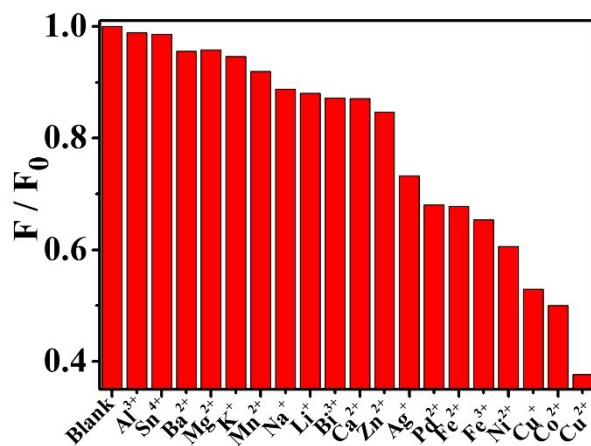


Fig. S16 Fluorescence responses of the PVIm dots to different metal ions at concentration of $80.0 \mu\text{M}$, respectively. PVIm dots: 0.2 mg mL^{-1} , $\lambda_{\text{ex}} = 320 \text{ nm}$.

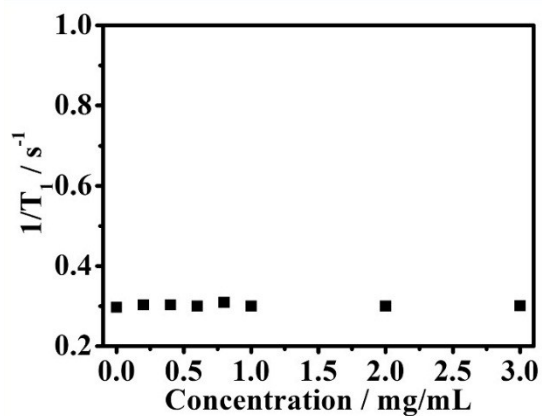


Fig. S17 Plots of $1/T_1$ vs. PVIm dots. T_1 values were obtained at 0, 0.2, 0.4, 0.6, 0.8, 1, 2, and 3 mg mL^{-1} aqueous solution of the PVIm dots, respectively.

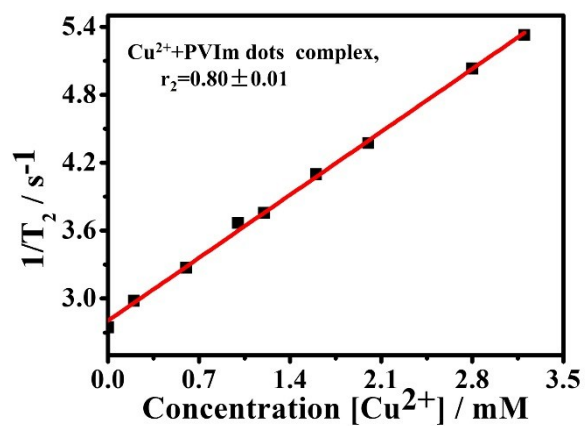


Fig. S18 Plots of $1/T_2$ vs. concentration of Cu^{2+} added to 0.2 mg mL^{-1} aqueous solution of PVIm dots to form complexes.